

# Fe<sub>3</sub>O<sub>4</sub>–SiO<sub>2</sub>–P4VP pH-Sensitive Microgel for Immobilization of Nickel Nanoparticles: An Efficient Heterogeneous Catalyst for Nitrile Reduction in Water

Mohammad Reza Nabid,\* Yasamin Bide, and Mahvash Niknezhad<sup>[a]</sup>

Fe<sub>3</sub>O<sub>4</sub> magnetic nanoparticles (MNPs) were modified with (3-aminopropyl)triethoxysilane through silanization. An atom transfer radical polymerization-initiating site immobilized onto amine-functionalized Fe<sub>3</sub>O<sub>4</sub> MNPs. The surface-initiated atom transfer radical polymerization of 4-vinylpyridine was then performed in the presence of Fe<sub>3</sub>O<sub>4</sub>–SiO<sub>2</sub>–Br nanoparticles, which led to the formation of Fe<sub>3</sub>O<sub>4</sub>–SiO<sub>2</sub>–P4VP [P4VP = poly(4-vinylpyridine)] hybrid microgels cross-linked with Fe<sub>3</sub>O<sub>4</sub> MNPs. Our approach uses polymer microgels as templates for the synthesis of nickel nanoparticles (NiNPs). The tunable properties of

synthesized NiNPs@Fe<sub>3</sub>O<sub>4</sub>–SiO<sub>2</sub>–P4VP pH-sensitive microgels were used in the catalytic reduction of aliphatic and aromatic nitriles. Moreover, the catalytic activity of metal nanocomposites that can be modulated by the volume transition of microgel structures with changing pH has been evaluated. TEM, X-ray photoelectron spectroscopy, thermogravimetric analysis, atomic absorption spectroscopy, XRD, UV/Vis spectroscopy, and FTIR spectroscopy were used to characterize the resultant catalyst.

## Introduction

Amines are important in various industries, such as plastics, dyes, agrochemicals, surfactants, and auxiliaries in the rubber and paper industries, and as anticorrosion agents, organic building blocks, and intermediates for material science. Owing to their interesting properties, amines are important functionalities in academic and industrial research.<sup>[1–8]</sup> For example, the worldwide production of aliphatic amines in 2000 was several lakh tons per annum.<sup>[9]</sup> Moreover, the growing use of biologically relevant nitrogenous molecules has necessitated the development of new and efficient methods to prepare amines.<sup>[10–13]</sup> Of many methods developed to synthesize amines, the most general and often benign processes involve catalytic reductions.<sup>[14–18]</sup> The reduction of nitriles is an attractive method, owing to the commercial availability of nitriles and the high atom efficiency of these reductions. Reported methods for the reduction of C–N multiple bonds include catalytic hydrogenation with LiAlH<sub>4</sub> and NaBH<sub>4</sub>. However, these methods are not general and have some drawbacks that confine them to reducing only some of these C–N multiple bond compounds.<sup>[19,20]</sup> For example, often a mixture of primary, secondary, and tertiary amines is obtained through the catalytic hydrogenation of C–N multiple bonds. Some disadvantages of using LiAlH<sub>4</sub> are decreased selectivity and low yields, owing to


the formation of colloidal materials upon workup and its high sensitivity to water. NaBH<sub>4</sub> can be efficient in the presence of a Lewis acid<sup>[21]</sup> such as LiCl,<sup>[22]</sup> TiCl<sub>4</sub>,<sup>[23]</sup> TiCl<sub>3</sub>,<sup>[24]</sup> or ZrCl<sub>4</sub>.<sup>[25,26]</sup> Moreover, the high hydrogen content, safe handling, environmentally benign properties, and stability of boron hydrides have increased the attention to these compounds.<sup>[27]</sup> The use of a suitable transition metal as a heterogeneous catalyst can increase the reducing power of NaBH<sub>4</sub> and lead to the development of mild, more selective, and practical methods for the reduction of the C–N multiple bonds to amino groups.<sup>[28–34]</sup>

Nanosized catalysts can efficiently improve heterogeneous catalytic reactions in organic synthesis.<sup>[35–40]</sup> In the reduction reactions, the first-row transition metals are much more attractive as catalysts than the precious metals, owing to their less cost and abundance in the earth. Nickel-based nanosized catalysts have been used for the reduction of aldehydes and ketones,<sup>[41]</sup> for the hydrogenation of olefins<sup>[42,43]</sup> and as supports for hydrogen adsorption,<sup>[44]</sup> and so on.

However, to prevent the aggregation of metal nanoparticles in a solution, they must be stabilized in suitable carrier systems. Dendrimers,<sup>[45,46]</sup> block copolymer micelles,<sup>[47]</sup> microgels (MGs),<sup>[48–51]</sup> and latex particles<sup>[52,53]</sup> are used as “nanoreactors” in which the metal nanoparticles can be immobilized and used for the desired purpose. Of these systems, MGs have several important advantages, such as stability, straightforward synthesis, and facile functionalization to provide stimuli-responsive behavior (e.g., change in volume in response to a change in temperature, pH, or ionic strength).<sup>[49]</sup>

For typical types of organic–inorganic hybrid MGs, the easiest synthesis approach that does not need any conventional chemical cross-linker is in situ formation of hybrid MGs via covalent cross-linking with functional inorganic nanoparticles

[a] Dr. M. R. Nabid, Y. Bide, M. Niknezhad  
Faculty of Chemistry  
Department of Polymer  
Shahid Beheshti University  
G.C., P.O. Box 1983963113, Tehran (Iran)  
Fax: (+98)21-22431661  
E-mail: m-nabid@sbu.ac.ir

 Supporting information for this article is available on the WWW under <http://dx.doi.org/10.1002/cctc.201300984>.

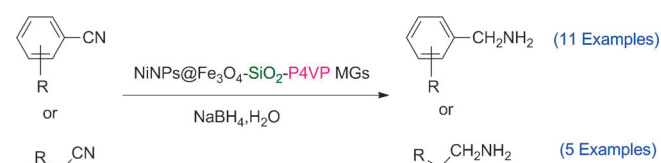
that actually act as chemical cross-linkers. At present, only a few reports exist about this type of organic–inorganic hybrid MGs. Magnetic nanoparticles (MNPs) have the added advantage of being magnetically separable and thus eliminated the requirement of the catalyst filtration after the reaction completion.

Because of our interest in the use of catalysts in the development of useful new synthesis methodologies<sup>[54–57]</sup> as well as the general importance of this issue, we present the synthesis and characterization of nickel nanoparticles immobilized on  $\text{Fe}_3\text{O}_4\text{-SiO}_2\text{-P4VP}$  [P4VP = poly(4-vinylpyridine)] pH-sensitive MGs ( $\text{NiNPs@Fe}_3\text{O}_4\text{-SiO}_2\text{-P4VP}$  MGs) and their use as heterogeneous catalysts for the reduction of aliphatic and aromatic nitriles to form primary amines with a broad substrate scope (Scheme 1).

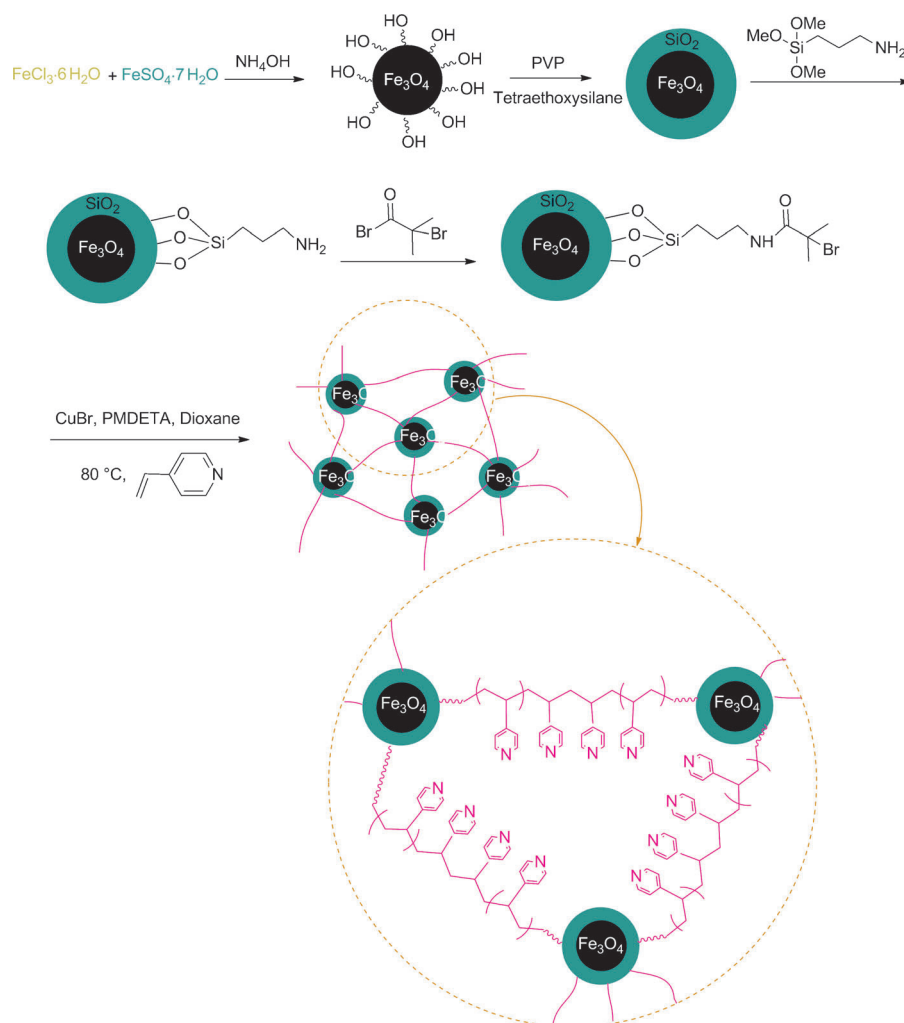
## Results and Discussion

### Synthesis and characterization of the supported catalyst

The synthesis method of  $\text{Fe}_3\text{O}_4\text{-SiO}_2\text{-P4VP}$  organic–inorganic hybrid MGs consists of a “grafting from” strategy via the atom transfer radical polymerization (ATRP) reaction, which involves the following steps (Scheme 2): 1) MNPs of 8–12 nm were synthesized with the method described by Sahu et al., which involves coprecipitation of  $\text{Fe}^{2+}$  and  $\text{Fe}^{3+}$  with the ammonium hydroxide solution.<sup>[58]</sup> 2) Owing to the aggregation of nanoparticles and solubility problems in organic media, our initial attempts to synthesize MGs, directly on the MNPs, failed. Coating MNPs with silica could solve these problems. For this purpose, after coating with polyvinylpyrrolidone (PVP), MNPs were suspended in 2-propanol and mixed with tetraethoxysilane to create a silica shell under basic conditions by using a sol–gel



**Scheme 1.**  $\text{NiNPs@Fe}_3\text{O}_4\text{-SiO}_2\text{-P4VP}$  MGs as the catalyst system for the reduction of nitriles.

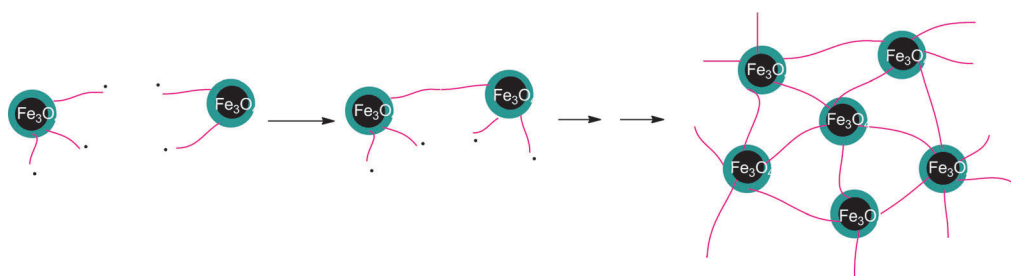


**Scheme 2.** Synthesis of  $\text{Fe}_3\text{O}_4\text{-SiO}_2\text{-P4VP}$  MGs (N,N,N',N',N''-pentamethyldiethylenetriamine = PMDETA).

process.<sup>[59]</sup> 3) The surface silanation of these silica-coated nanoparticles with (3-aminopropyl)triethoxysilane under reflux conditions in toluene for 24 h gave  $0.37 \text{ mmol g}^{-1}$  of amino groups (determined by using back titration). 4) 2-Bromoisobutyryl bromide (BIBB), an ATRP-initiating site, immobilized onto amino-functionalized magnetic  $\text{Fe}_3\text{O}_4$  MNPs by nucleophilic attack of the amino group to acyl bromide of BIBB. 5)  $\text{Fe}_3\text{O}_4\text{-SiO}_2\text{-P4VP}$  MGs were synthesized with  $\text{Fe}_3\text{O}_4\text{-SiO}_2\text{-Br}$  nanoparticles as cross-linkers and 4VP as the monomer through the ATRP reaction (Scheme 2). The living radical polymerization enables the coating of the polymer on the  $\text{Fe}_3\text{O}_4$  surface in a controlled fashion, which results in good dispersibility of the particles in a suitable medium. The synthesized polymeric network involving  $\text{Fe}_3\text{O}_4$  MNPs as cross-linking points is formed through interparticle termination reactions of the growing free radicals situated on neighboring  $\text{Fe}_3\text{O}_4$  MNPs (Scheme 3).

Then,  $\text{Ni}^{2+}$  ions were introduced into  $\text{Fe}_3\text{O}_4\text{-SiO}_2\text{-P4VP}$  MGs and subsequently reduced with sodium borohydride to obtain  $\text{NiNPs@Fe}_3\text{O}_4\text{-SiO}_2\text{-P4VP}$  MGs (Scheme 4).

The FTIR spectra of  $\text{Fe}_3\text{O}_4$  MNPs, PVP-coated  $\text{Fe}_3\text{O}_4$  MNPs, silica-coated  $\text{Fe}_3\text{O}_4$  MNPs,  $\text{Fe}_3\text{O}_4\text{-SiO}_2\text{-NH}_2$ , and  $\text{Fe}_3\text{O}_4\text{-SiO}_2\text{-Br}$



**Scheme 3.** Schematic of interparticle termination giving a cross-linked network.

are shown in Figure S1 a–e, respectively. Moreover,  $\text{Fe}_3\text{O}_4\text{-SiO}_2\text{-P4VP}$  MGs were characterized by using FTIR spectroscopy (Figure 1). The pyridine ring signals appeared at  $1661\text{ cm}^{-1}$ . In addition, the peak at  $1220\text{ cm}^{-1}$  is assigned to the aromatic amine of the pyridyl rings. Moreover, the characteristic signals of pyridyl rings, such as out-of-plane deformation vibrations of 4-monoalkyl pyridine ( $818\text{ cm}^{-1}$ ) and hydrogen bending of 4-monosubstituted pyridine ( $1024\text{ cm}^{-1}$ ), were also apparent, which indicated the existence of P4VP. Thus, the FTIR spectra confirmed the formation of  $\text{Fe}_3\text{O}_4\text{-SiO}_2\text{-P4VP}$  MGs.

The TEM observation indicates that  $\text{Fe}_3\text{O}_4\text{-SiO}_2\text{-P4VP}$  MGs and  $\text{NiNPs@Fe}_3\text{O}_4\text{-SiO}_2\text{-P4VP}$  MGs contained many small black

spheres, which were  $\text{Fe}_3\text{O}_4$  MNPs (Figure 2a and b). The TEM images confirmed that  $\text{Fe}_3\text{O}_4$  MNPs act as cross-linkers. BIBB-modified  $\text{Fe}_3\text{O}_4$  MNPs are like chemical cross-linkers with multi-

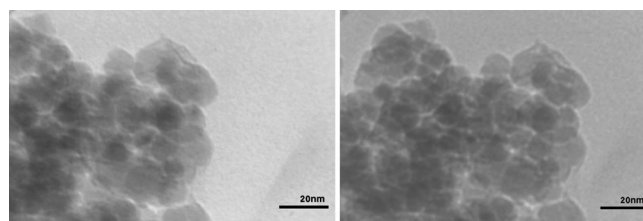


**Figure 2.** TEM images of  $\text{NiNPs@Fe}_3\text{O}_4\text{-SiO}_2\text{-P4VP}$  MGs.

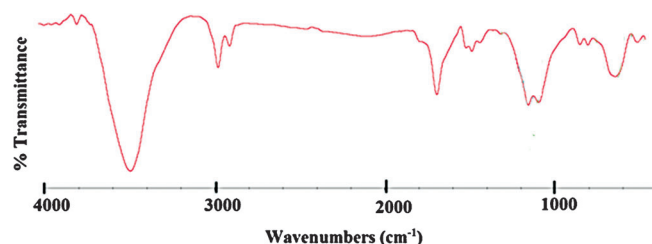
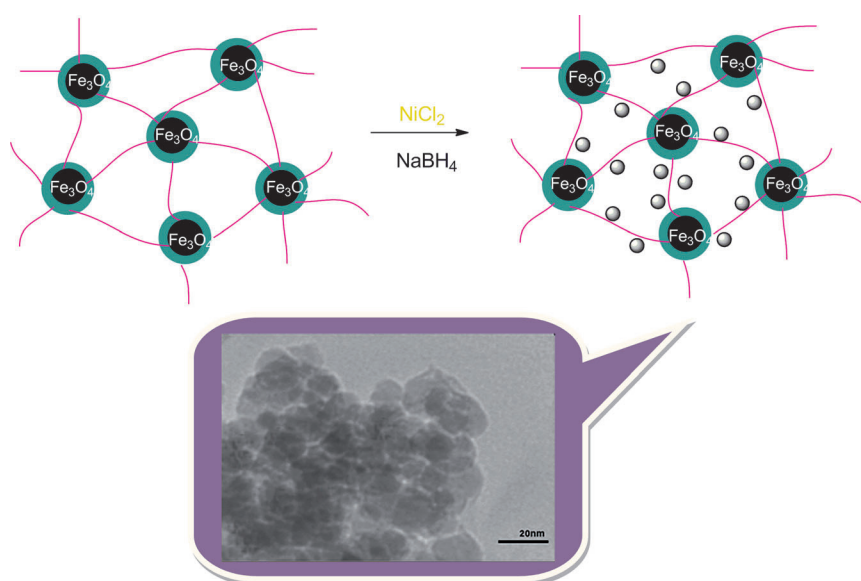


**Figure 1.** FTIR spectrum of  $\text{Fe}_3\text{O}_4\text{-SiO}_2\text{-P4VP}$  MGs.

ple functional groups, which led to the successful formation of hybrid MGs. Furthermore, the TEM images of  $\text{NiNPs@Fe}_3\text{O}_4\text{-SiO}_2\text{-P4VP}$  MGs (Figure 2b) show that nickel nanoparticles were uniformly dispersed on  $\text{Fe}_3\text{O}_4\text{-SiO}_2\text{-P4VP}$  MGs, in which the main average size of nickel nanoparticles is approximately 2–4 nm. This observation is attributable to the existence of a large number of nitrogen-containing pyridine groups as anchoring sites on the  $\text{Fe}_3\text{O}_4$  surface.

The UV/Vis spectra of  $\text{Fe}_3\text{O}_4\text{-SiO}_2$ ,  $\text{Fe}_3\text{O}_4\text{-SiO}_2\text{-NH}_2$ ,  $\text{Fe}_3\text{O}_4\text{-SiO}_2\text{-P4VP}$  MGs, and  $\text{NiNPs@Fe}_3\text{O}_4\text{-SiO}_2\text{-P4VP}$  MGs are shown in Figure 3 a–d, respectively. In the spectra of  $\text{Fe}_3\text{O}_4\text{-SiO}_2$  and  $\text{Fe}_3\text{O}_4\text{-SiO}_2\text{-NH}_2$ , a broad featureless peak can be observed at a wavelength of approximately 390 nm, which confirms the core-shell  $\text{Fe}_3\text{O}_4\text{-SiO}_2$  MNPs and may result from the changes in band gap caused by the quantum size effect and the surface effect of nanostructures<sup>[60,61]</sup> and the Fe–O–Si bonds of the core-shell nanoparticles.<sup>[62]</sup> The UV/Vis spectrum of  $\text{Fe}_3\text{O}_4\text{-SiO}_2\text{-P4VP}$  MGs demonstrates a broad absorption band at approximately 257 nm. This band was assigned to pyridine ring absorption, and



**Scheme 4.** Synthesis of  $\text{NiNPs@Fe}_3\text{O}_4\text{-SiO}_2\text{-P4VP}$  MGs.

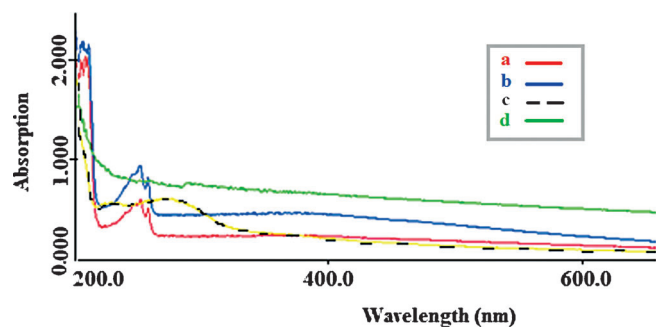


**Figure 3.** UV/Vis spectra of a)  $\text{Fe}_3\text{O}_4\text{-SiO}_2$  (red), b)  $\text{Fe}_3\text{O}_4\text{-SiO}_2\text{-NH}_2$  (blue), c)  $\text{Fe}_3\text{O}_4\text{-SiO}_2\text{-P4VP}$  MGs (yellow), and d)  $\text{NiNPs@Fe}_3\text{O}_4\text{-SiO}_2\text{-P4VP}$  MGs (green).

its structured feature can be attributed to both  $\pi \rightarrow \pi^*$  and  $n \rightarrow \pi^*$  transitions that are located in the same spectral region. The spectrum of  $\text{NiNPs@Fe}_3\text{O}_4\text{-SiO}_2\text{-P4VP}$  MGs shows absorption bands at 211 nm and a shoulder at 310 nm, which is probably due to the effect of quantum size for this particle size (2–4 nm). These results are in agreement with the values reported by the work of Creighton and Eadon,<sup>[63]</sup> in which particles with a size of 10 nm show a band near 210 nm. Curtis et al. found that the absorption of the bulk nickel presents a band centered near 230 nm.<sup>[64]</sup>

Thermogravimetric analysis (TGA) was performed for the quantitative analysis of functionalized  $\text{Fe}_3\text{O}_4$  MNPs. Before TGA measurements, freely adsorbed P4VP molecules were removed through Soxhlet extraction with boiling methanol for 36 h. The TGA curves of silica-coated magnetite nanoparticles,  $\text{Fe}_3\text{O}_4\text{-SiO}_2\text{-P4VP}$  MGs, and  $\text{NiNPs@Fe}_3\text{O}_4\text{-SiO}_2\text{-P4VP}$  MGs are shown in Figure S2A–C. According to the TGA results, the content of nickel in the synthesized catalyst is approximately 12 wt%, which is in good agreement with the atomic absorption spectroscopy data.

The XRD patterns of  $\text{Fe}_3\text{O}_4$  MNPs,  $\text{Fe}_3\text{O}_4\text{-SiO}_2$ , and  $\text{Fe}_3\text{O}_4\text{-SiO}_2\text{-P4VP}$  MGs are shown in Figure S3, which indicate that the crystal structure of  $\text{Fe}_3\text{O}_4$  during the synthesis of the magnetic MG is well maintained.

X-ray photoelectron spectroscopy (XPS) is a powerful tool for the investigation of hybrid materials. The XPS spectrum of  $\text{NiNPs@Fe}_3\text{O}_4\text{-SiO}_2\text{-P4VP}$  MGs (Figure 4) demonstrates the photoelectron lines at binding energies of approximately 285, 531, and 711 eV, which are attributed to C1s, O1s, and Fe2p, respectively. In contrast to the  $\gamma\text{-Fe}_2\text{O}_3$  XPS spectrum, it does not contain the charge transfer satellite of  $\text{Fe}2p_{3/2}$  at 720 eV, which confirms that the oxide in the sample was  $\text{Fe}_3\text{O}_4$ .<sup>[65]</sup> The nitrogen (N1s) signal is attributed to P4VP and PVP produced during the synthesis of  $\text{NiNPs@Fe}_3\text{O}_4\text{-SiO}_2\text{-P4VP}$  MGs. The peak at 103 eV is assigned to Si2p, which indicates that  $\text{SiO}_2$  is deposited on the  $\text{Fe}_3\text{O}_4$  surface.

The spectrum of the Ni2p core level of  $\text{NiNPs@Fe}_3\text{O}_4\text{-SiO}_2\text{-P4VP}$  MGs is shown in Figure 5, which demonstrates two bands at 863 and 881 eV assigned to  $\text{Ni}^0 2p_{3/2}$  and  $\text{Ni}^0 2p_{1/2}$ , respectively. The relative intensities of the  $2p_{3/2}$  and  $2p_{1/2}$  peaks are approximately 1:2. The  $2p_{3/2}$  and  $2p_{1/2}$  binding energies are shifted to the higher values relative to the values for the bulk

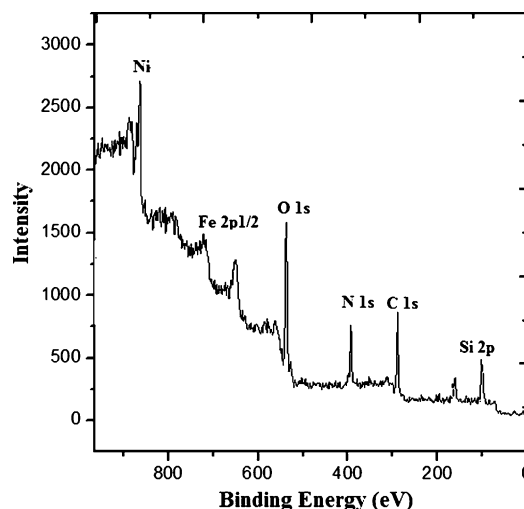


**Figure 4.** XPS spectrum of  $\text{NiNPs@Fe}_3\text{O}_4\text{-SiO}_2\text{-P4VP}$  MGs.

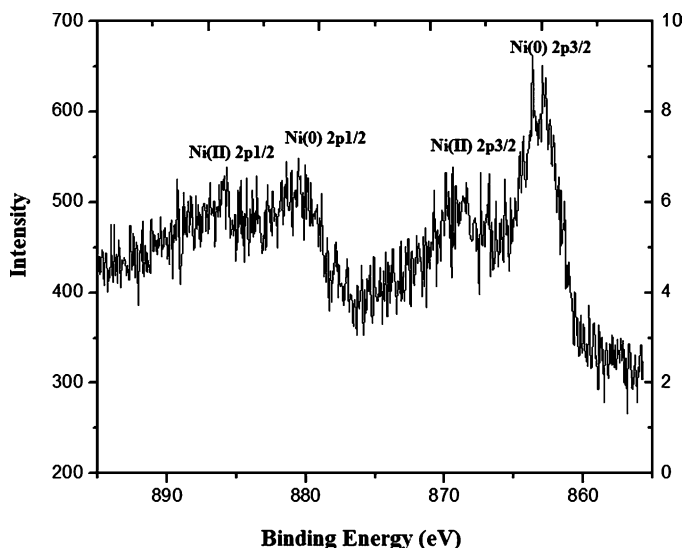


**Figure 5.** XPS spectrum of the Ni2p core level region for  $\text{NiNPs@Fe}_3\text{O}_4\text{-SiO}_2\text{-P4VP}$  MGs.

nickel (852.3 and 869.7 eV, respectively),<sup>[66]</sup> which can be attributed to the matrix effect.<sup>[67]</sup> XPS has been used to determine the oxidation states of nickel in the catalyst sample. The two peaks with lower intensities at 868 and 885 eV are related to  $\text{Ni}^{2+}$  species that could have been formed during the XPS sample preparation because the stabilized  $\text{Ni}^0$  nanoclusters are sensitive to aerobic atmosphere.

#### The catalytic activity and selectivity of $\text{NiNPs@Fe}_3\text{O}_4\text{-SiO}_2\text{-P4VP}$ MGs toward the reduction of nitriles

With nickel nanoparticles immobilized on  $\text{Fe}_3\text{O}_4\text{-SiO}_2\text{-P4VP}$  MGs in hand, we attempted to evaluate their catalytic activity for the reduction of nitriles. The reduction of benzonitrile was performed initially as a model reaction. To optimize the amount of the catalyst, the model reaction was performed

with various amounts of the catalyst in water at room temperature. Within 2 h and with 1 mol% of nickel, 88% isolated yield of benzyl amine was obtained (Table 1, entry 4). With 0.4 and 0.7 mol% of nickel, a longer time is required for the reaction to complete even under thermal conditions (80 °C) and it

**Table 1.** Effect of the amount of the catalyst on the reduction of benzonitrile.<sup>[a]</sup>

Entry	Amount of the catalyst (Ni <sup>0</sup> content) [mol%]	<i>t</i> [h]	<i>T</i> [°C]	Isolated yield [%]
1	0.4	3.5	80	46
2	0.7	3	25	68
3	0.7	2.2	80	77
4	1	2	25	88
5	1.1	2	25	89

[a] Reaction conditions: 1 mmol of benzonitrile, 1 mmol of NaBH<sub>4</sub>, 5 mL of water, NiNPs@Fe<sub>3</sub>O<sub>4</sub>-SiO<sub>2</sub>-P4VP MGs as the catalyst system, and pH adjusted to 5.5.

causes the reaction to occur with decreased yields (Table 1, entries 1–3). In contrast, increasing the amount of the catalyst to 1.1 mol% did not affect the yield considerably (Table 1, entry 5). In the next step, the effect of the solvent on the reaction was investigated (Table 2). The yield in water is significant-

**Table 2.** Effect of different solvents on the reduction of benzonitrile.<sup>[a]</sup>

Entry	Solvent	<i>T</i> [h]	Isolated yield [%]
1	acetonitrile	4	40
2	DMF	4	51
3	THF	5	38
4	toluene	5	28
5	water	2	88
6	<i>N</i> -methylpyrrolidone	2	62

[a] Reaction conditions: 1 mmol of benzonitrile, 1 mmol of NaBH<sub>4</sub>, 5 mL of the solvent, 25 °C, NiNPs@Fe<sub>3</sub>O<sub>4</sub>-SiO<sub>2</sub>-P4VP MGs as the catalyst system, and pH adjusted to 5.5.

ly higher than other solvents, owing to the hydrophobic nature of P4VP, which concentrates the substrates in its inner sites in which the nickel nanoparticles exist. Thus, the catalyst and substrates collect in the same sites and an efficient catalytic reaction occurs. Then, to investigate more about the catalytic event and to study the effect of pH, we used the reduction of benzonitrile in different pH values (Table 3 and Figure 6). A buffer solution of (0.1 M) KH<sub>2</sub>PO<sub>4</sub>/K<sub>2</sub>HPO<sub>4</sub> was used to maintain the pH values stable. The pH of the buffer solution was adjusted with HCl and NaOH at a certain amount. The results indicated that the reaction occurred efficiently at pH 5.5. However, at higher pH, the catalyst efficiency decreased significantly. At low pH, metal nanoparticles embedded in such a network are completely reachable by the reactants. However, above the transition, the diffusion of the reactants within the network

**Table 3.** Effect of pH on the reduction of benzonitrile with NiNPs@Fe<sub>3</sub>O<sub>4</sub>-SiO<sub>2</sub>-P4VP MGs as the catalyst system.<sup>[a]</sup>

Entry	pH	Yield [%]
1	4.5	31
2	5.5	88
3	6.5	22
4	7.5	20
5	8.5	17

[a] Reaction conditions: 1 mmol of benzonitrile, 1 mmol of NaBH<sub>4</sub>, 5 mL of water, 25 °C, NiNPs@Fe<sub>3</sub>O<sub>4</sub>-SiO<sub>2</sub>-P4VP MGs as the catalyst system, 2 h.

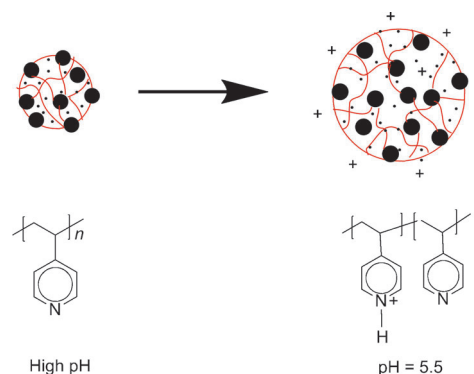


**Figure 6.** Fe<sub>3</sub>O<sub>4</sub>-SiO<sub>2</sub>-P4VP MGs as both the reaction medium and the metal catalyst support.

slows down, which is the result of the marked shrinking of the network. Thus, the rate of the reaction catalyzed by the nanoparticles decreases considerably. In this way, the network acts as a nanoreactor that can be opened or closed to a certain extent. Thus, the synthesized pH-sensitive MG system enables us to modulate the catalytic activity of MG-stabilized nanoparticles through a thermodynamic transition that takes place within the carrier system. Consequently, the best system for the reduction of benzonitrile is water as a solvent at room temperature with 1 mol% of nickel at pH 5.5. Thus, the results indicate that at pH 4.5 and lower pH values, most of the pyridine groups are protonated and the MG swells whereas at pH 6.5 and higher pH values, owing to the hydrophobic nature of pyridine groups, the hybrid MG deswells. At pH 5.5, pyridine groups that orient along outer regions of the MG are protonated to have interaction with water molecules in an aqueous medium; however, pyridine groups in the inner regions of the MG are not protonated, although partial swelling occurs and some water diffuses into the inner region. Partial swelling permits the MG to accept the substrates to the inner hydrophobic part, whereas in the deswelled form (pH > 5.5), the diffusion of substrates to the inner parts decreases owing to steric interactions. Thus, in the catalytic reaction in an aqueous medium, the organic substrates were ejected from the water medium and the hydrophilic outer region of the MG to concentrate in the inner hydrophobic regions, in which the metal catalysts exist and therefore an efficient catalytic reaction occurs.

To prove the efficiency of the catalyst, we studied the reduction reactions of different aliphatic and aromatic nitriles



(Table 4); the  $^1\text{H}$  NMR spectra of the products are shown in Figures S4–S20. Reductions of benzonitriles with one or more electron-withdrawing groups on the aromatic ring are generally faster and result in higher yields (Table 4, entries 4–11). For example, 2,4-dichlorobenzonitrile and 2-chloro-4-bromobenzonitrile were reduced to 2,4-dichlorobenzylamine and 2-chloro-4-bromobenzylamine in 99% yield (Table 4, entries 9 and 10). We found that benzonitriles with a sterically crowded nitrile (Table 4, entry 11) or electron-donating groups (Table 4, entries 2 and 3) required higher temperatures for the complete reduction. For example, 2,6-dichlorobenzonitrile was reduced to the corresponding amine in 88% yield after 1 h of refluxing in water (Table 4, entry 11). The lower yield and need for increased temperature is attributed to the steric hindrance around the reduction site. In addition, 4-methoxybenzonitrile is reduced to the corresponding 4-methoxybenzylamine in 89% yield after 1 h reflux in water. The reduction of 4-cyanobenzaldehyde lead to [4-(aminomethyl) phenyl]methanol in 90% yield, in which both the nitrile and the aldehyde groups were reduced (Table 4, entry 5). Thus, the selective reduction of a nitrile in the presence of an aldehyde group was not successful. Aliphatic nitriles can also be reduced with  $\text{NiNPs}@Fe_3O_4\text{-SiO}_2\text{-P4VP}$  MGs as the catalyst system. Notably, many of the current systems cannot reduce aliphatic nitriles even under extended reflux conditions,<sup>[68–70]</sup> owing to the deprotonation of the hydrogen  $\alpha$  to the nitrile with these reagents and thus halting the reduction. However, our catalytic system does not suffer from this problem and several aliphatic nitriles were reduced to their analogous amines in refluxing water in excellent yields (Table 4, entries 12–15). Benzyl cyanides are hard nitriles to reduce, owing to the extreme acidity of the protons  $\alpha$  to the nitrile and consequently deprotonation instead of reduction with most reducing agents. In contrast, the

Entry	Nitrile	Amine	T [°C]	t [h]	Conversion [%]	Isolated yield [%]	Selectivity <sup>[b]</sup> [%]
1			25	2	90	88	98
2			100	1	91	90	98
3			100	1	91	89	97
4			25	2	> 99	99	> 99
5			25	2	93	90	96
6			25	2	97	94	97
7			25	2	94	93	98
8			25	2	93	93	> 99
9			25	2	> 99	99	> 99
10			25	2	> 99	99	> 99
11			100	1	88	88	> 99
12			100	18	90	87	96
13			100	12	95	92	97
14			100	12	89	87	98
15			100	8	98	97	99
16			100	7	89	86	96
17 <sup>[c]</sup>			25	3	99	99	> 99
18 <sup>[d]</sup>			25	2	79	74	95
19 <sup>[e]</sup>			25	2	87	83	96

[a] Reaction conditions: 1 mmol of nitrile, 1 mmol of  $\text{NaBH}_4$ , 5 mL of water,  $\text{NiNPs}@Fe_3O_4\text{-SiO}_2\text{-P4VP}$  MGs (1 mol% of  $\text{Ni}^0$ ) as the catalyst system, and pH adjusted to 5.5; [b] Calculated selectivity; [c] 1 mmol of dinitrile and 2 mmol of  $\text{NaBH}_4$ ; [d] Alternate conditions:  $\text{H}_2$  was used instead of  $\text{NaBH}_4$ , 0.4 MPa; [e] Alternate conditions:  $\text{H}_2$  was used instead of  $\text{NaBH}_4$ , 0.6 MPa.

presented catalyst reduces several examined benzyl cyanides to their corresponding phenethylamines in excellent yields.

The reduction of benzyl cyanides is an important issue because it enables the facile preparation of various biologically active compounds from similar benzyl nitriles. An aliphatic nitrile that contains an alkyne not conjugated with the nitrile group was tested and showed that the nitrile group can be reduced selectively without affecting the C–C multiple bond

(Table 4, entry 16). Terephthalonitrile as a dinitrile was also examined, which gave 1,4-phenylenedimethanamine with excellent yield (Table 4, entry 17).

In addition, in our catalytic system, the special structure of the supported catalyst that helps determine the surface of the catalyst is the reason for the high selectivity of this system.

Steric effects avoid the formation of secondary and tertiary amines. Similarly, the high retention of the triple bonds can be attributed to steric effects and the preference that these effects have for the absorption of the nitrile over that of the triple bonds. Moreover, with respect to the general applicability of the NiNPs@Fe<sub>3</sub>O<sub>4</sub>-SiO<sub>2</sub>-P4VP catalyst, we tested the hydrogenation of benzonitrile with molecular hydrogen as a model reaction, which is especially important from the economic and ecological viewpoints, and the results are shown in Table 4 (entries 18 and 19).

Thus, we have achieved several important objectives: 1) having a heterogeneous catalyst bearing the advantage of being magnetically separable and thus removing the need of the catalyst filtration after the reaction completion; 2) using MGs as stabilizers for nanoparticles, which have several important advantages such as stability, straightforward synthesis, and facile functionalization; 3) forming hybrid MGs in situ via covalent cross-linking with functional inorganic nanoparticles that does not need any conventional chemical cross-linker; 4) providing the stimuli-sensitive support, which changes in volume with the change in pH; in reality, the physicochemical properties of the polymeric MG significantly affect the catalytic activity; and 5) developing an efficient synthesis process for the facile and selective catalytic reduction of aliphatic and aromatic nitriles.

### Recycling NiNPs@Fe<sub>3</sub>O<sub>4</sub>-SiO<sub>2</sub>-P4VP MGs

Many reports of stable and recyclable supported homogeneous catalysts confirm the catalyst stability and recyclability on the basis of a single data point in each run and often a reaction yield after a long reaction time. However, catalysis is completely a kinetic phenomenon, and thus one can argue that only kinetic data should be considered to confirm recyclability, stability, and deactivation. The measurement of initial rates obtained from kinetic plots is a good approach to investigate recyclability and deactivation because if a single data point was taken in each run after a long reaction time, one could incorrectly conclude that the catalyst is completely stable and recyclable.<sup>[71]</sup> Thus, we investigate conversion yields for every run after 30 min for the reduction of benzonitrile as a model reaction. The reaction was monitored by using GC, and the results are shown in Figure 7. Analysis of NiNPs@Fe<sub>3</sub>O<sub>4</sub>-SiO<sub>2</sub>-P4VP MGs revealed good stability and recyclability, as the conversion yields for seven runs after 30 min did not decrease significantly. In addition, to investigate the productivity of the prepared catalyst, we examined the reduction of benzonitrile for seven cycles even after the completion of the reaction. The results shown in Figure 7b demonstrate that after every run, the product yield does not change significantly, which indicates the high productivity of the catalyst.

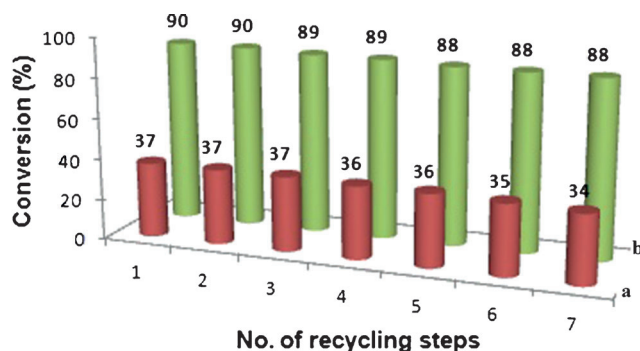


**Figure 7.** Effect of recycling on the catalytic activity and productivity of NiNPs@Fe<sub>3</sub>O<sub>4</sub>-SiO<sub>2</sub>-P4VP MGs after a) 30 min (red) and b) 2 h (green).

Notably, magnetic extraction precludes the need for filtration or centrifugation steps and the workup of the final reaction mixture to recover the catalyst.

### Conclusions

The pH-sensitive organic-inorganic hybrid microgels [Fe<sub>3</sub>O<sub>4</sub>-SiO<sub>2</sub>-P4VP MGs; P4VP = poly(4-vinylpyridine)] were prepared through the surface-initiated atom transfer radical polymerization with 4VP as the pH-sensitive monomer and Fe<sub>3</sub>O<sub>4</sub> magnetic nanoparticles as cross-linkers. The formation of the synthesized magnetic MG was confirmed by using FTIR, UV/Vis, thermogravimetric analysis, XRD, and X-ray photoelectron spectroscopy analysis. The synthesized hybrid MGs were effectively used as substrates for the in situ formation of nickel nanoparticles (NiNPs). The encapsulation of NiNPs on Fe<sub>3</sub>O<sub>4</sub>-SiO<sub>2</sub>-P4VP MGs was studied confirmatively by using atomic absorption spectroscopy, thermogravimetric analysis, XRD, X-ray photoelectron spectroscopy, and TEM. The prepared NiNPs@Fe<sub>3</sub>O<sub>4</sub>-SiO<sub>2</sub>-P4VP MGs were used as new nanocatalysts for the reduction of various nitriles. Both aromatic and aliphatic nitriles can be reduced with this catalyst in high yields. The recyclability of the catalyst was examined for seven cycles, which showed no loss in activity. This system has the advantages of flexibility and practicality, a simple workup process, and easy recovery of the catalyst, and thus it can be used for the reduction of many different C–N multiple bonds.

### Experimental Section

#### Materials

FeCl<sub>3</sub>·6H<sub>2</sub>O and FeSO<sub>4</sub>·7H<sub>2</sub>O were purchased from Merck. Ammonium hydroxide was received from Merck. (3-Aminopropyl)triethoxysilane was purchased from Acros Organics. Toluene was dried over sodium. Dichloromethane and methanol were dried from calcium hydride and magnesium, respectively. 4VP (95%, Acros) was fractionally distilled before use. Nickel(II) chloride, PVP (65 000 Da), and BIBB were purchased from Merck. All other solvents and reagents were purchased from Aldrich or Merck and used without further purification unless otherwise stated.

## Instruments and characterization

The IR spectra were recorded on a BOMEM MB-Series FT-IR spectrophotometer. The  $^1\text{H}$  NMR spectra were recorded on a Bruker AVANCE DRX-300 spectrometer, and deuterated chloroform was used as a solvent. The TEM images were recorded with a LEO 912AB electron microscope. Catalysis products were analyzed with a Varian 3900 GC system (GC conversions were obtained with *n*-decane as an internal standard based on the amount of nitriles used relative to the authentic standard product). Ultrasonic bath (Eurosonic 4D ultrasonic cleaner with a frequency of 50 kHz and an output power of 350 W) was used to disperse materials in solvents. TGA was performed with an STA 1500 instrument at a heating rate of  $10^\circ\text{C min}^{-1}$  in air. The XRD patterns were collected on an XD-3A X-ray diffractometer using  $\text{CuK}\alpha$  radiation. XPS analysis was performed with a VG MultiLab 2000 spectrometer (Thermo VG Scientific) in an ultrahigh vacuum. The UV/Vis spectra were obtained with a Shimadzu UV-2100 spectrophotometer. CHN analysis was done with a Vario EL analyzer.

## Preparation and coating of the magnetite nanoparticles with silica

$\text{Fe}_3\text{O}_4$  MNPs were prepared by coprecipitating iron(II) and iron(III) in the alkaline solution according to the method described in the literature.<sup>[58]</sup> In brief,  $\text{FeCl}_3 \cdot 6\text{H}_2\text{O}$  (0.54 g) and  $\text{FeSO}_4 \cdot 7\text{H}_2\text{O}$  (0.3 g) were added to Millipore water (40 mL) under argon atmosphere. The aqueous ammonia solution (1.5 M) was introduced into the reaction vessel with violent stirring. Then, the reaction mixture was heated at  $80^\circ\text{C}$  and the pH of the medium was maintained at 10 with the addition of aqueous ammonium hydroxide (2.5 M) during the reaction. The obtained magnetite was immediately washed five times with water and then two times with ethanol. Then, MNPs were separated with an external magnet and were dried in a vacuum oven at  $50^\circ\text{C}$ . Coating of the nanoparticles with PVP was done according to the method of Lee and co-workers.<sup>[72]</sup> A solution of PVP-coated magnetite nanoparticles (1 g) was suspended in 2-propanol (2 L) containing concentrated ammonia (50 mL, 28%).

The solution was divided into three portions, and each one was sonicated for 1 h. After combining the solutions, tetraethoxysilane (5 mL, 22.4 mmol) in 2-propanol (100 mL) was added dropwise, over a 3 h period, to the magnetite solution under mechanical stirring. The stirring was continued for another 3 h, and then the silica-coated nanoparticles were separated magnetically after the decantation of the solution and washed three times with time drinking water (TDW). The final product was obtained after drying at RT for 24 h under a vacuum of 0.2 mmHg.

## Silanation of the silica-coated magnetite nanoparticles

Dry silica-coated magnetite powder (10 g) was suspended in dry toluene (200 mL). After sonication for 35 min, a solution of (3-aminopropyl)triethoxysilane (2.5 mL, 10.68 mmol) was added under mechanical stirring. The solution was heated at  $105^\circ\text{C}$  for 20 h. The particles were separated with an external magnet after cooling to RT, washed three times with dry methanol, and dried under vacuum for 24 h. Amino groups ( $0.37 \text{ mmol g}^{-1}$ ) were found (as determined by using back titration and CHN analysis methods, which are in good agreement with each other).

## Preparation of BIBB-coated MNPs

The amine-modified  $\text{Fe}_3\text{O}_4\text{-SiO}_2$  MNPs were dispersed in anhydrous dichloromethane (50 mL). After the addition of distilled triethylamine (0.711 mL, 5.0 mmol), the whole solution was kept in an ice bath under argon atmosphere and cooled to  $0^\circ\text{C}$ . BIBB (0.528 mL, 4.2 mmol) was added to the above solution, which was mechanically stirred for 2.0 h at  $0^\circ\text{C}$  and then at RT for 16 h. The synthesized MNPs (labeled as BIBB-coated MNPs) were isolated and washed three times with dichloromethane, ethanol, and water, respectively, and finally dried in vacuum overnight at  $50^\circ\text{C}$ .

## Surface-initiated ATRP of 4VP from BIBB-coated MNPs

The BIBB-coated MNPs (0.1 g) were sonicated with 4VP (3 mL, 28 mmol) in a Schlenk tube for 1 h before the addition of a solution of copper(II) bromide (0.3 g, 2.1 mmol) and  $\text{N,N,N',N'}$ -pentamethyldiethylenetriamine (PMDETA) (0.42 mL, 2.1 mmol) in dioxane (1 mL). The mixture was degassed by three freeze-pump-thaw cycles and heated at  $80^\circ\text{C}$  for 24 h to establish the ATRP reaction.  $\text{Fe}_3\text{O}_4\text{-SiO}_2\text{-P4VP}$  MGs were magnetically separated and washed thoroughly with methanol and dried in vacuum (Scheme 2).

## Preparation of $\text{NiNPs@Fe}_3\text{O}_4\text{-SiO}_2\text{-P4VP}$ MGs

The aqueous solution of nickel(II) chloride (0.01 mL, 0.15 M) and  $\text{Fe}_3\text{O}_4\text{-SiO}_2\text{-P4VP}$  MGs (0.1 g in 10 mL) were mixed and placed in an ultrasonic bath (50 kHz) for 10 min to disperse metal ions in the hybrid material. The mixture was stirred at RT for 8 h, and then reduction was performed with the addition of the aqueous solution of  $\text{NaBH}_4$  (0.5 mL, 0.01 M) to the mixture and stirring at RT for 1 h. It was filtered under vacuum, washed with ethanol and water ( $2 \times 20 \text{ mL}$ ), and dried under vacuum at  $50^\circ\text{C}$  for 4 h to obtain  $\text{NiNPs@Fe}_3\text{O}_4\text{-SiO}_2\text{-P4VP}$  MGs (Scheme 3). The atomic absorption spectroscopy and TGA were used to determine the amount of nickel in the synthesized catalyst.

## General method for the reduction of a nitrile with $\text{NiNPs@Fe}_3\text{O}_4\text{-SiO}_2\text{-P4VP}$ MGs as the catalyst system

A nitrile (1 mmol) was added to distilled water (2 mL), and then the ultrasonically dispersed  $\text{NiNPs@Fe}_3\text{O}_4\text{-SiO}_2\text{-P4VP}$  MG catalyst (0.005 g, 1 mol% of nickel) in water (3.0 mL) was added to this solution. Finally,  $\text{NaBH}_4$  (1 mmol, 0.038 g) was added. The mixture was stirred. After the reaction completion, the catalyst was removed with an external magnet and washed twice with dichloromethane (6.0 mL). Then, the organic phase was combined and the solvent was removed under vacuum to afford the pure product.

## Acknowledgements

We are grateful to Shahid Beheshti University Research Council for partial financial support of this work.

**Keywords:** nanoparticles • nickel • microgels • nitriles

[1] J. Seayad, A. Tillack, C. G. Hartung, M. Beller, *Adv. Synth. Catal.* **2002**, *344*, 795–813.

[2] F. Pohlki, S. Doye, *Chem. Soc. Rev.* **2003**, *32*, 104–114.

[3] W. Tang, X. Zhang, *Chem. Rev.* **2003**, *103*, 3029–3069.



- [4] N. Fleury-Brégeot, V. de La Fuente, S. Castellón, C. Claver, *ChemCatChem* **2010**, *2*, 1346–1371.
- [5] R. Severin, S. Doye, *Chem. Soc. Rev.* **2007**, *36*, 1407–1420.
- [6] T. E. Müller, K. C. Hultsch, M. Yus, F. Foubelo, M. Tada, *Chem. Soc. Rev.* **2008**, *37*, 3795–3892.
- [7] T. C. Nugent, M. El-Shazly, *Adv. Synth. Catal.* **2010**, *352*, 753–819.
- [8] M. Rueping, E. Sugiono, F. R. Schoepke, *Synlett* **2010**, *6*, 852–865.
- [9] J. Mielby, S. Kegnæs, P. Fristrup, *ChemCatChem* **2012**, *4*, 1037–1047.
- [10] Ö. F. Erdem, L. Schwartz, M. Stein, A. Silakov, S. Kaur-Ghumaan, P. Huang, S. Ott, E. J. Reijerse, W. Lubitz, *Angew. Chem.* **2011**, *123*, 1475–1479; *Angew. Chem. Int. Ed.* **2011**, *50*, 1439–1443.
- [11] P. Moschou, J. Wu, A. Cona, P. Tavladoraki, R. Angelini, K. Roubelakis-Angelakis, *J. Exp. Bot.* **2012**, *63*, 5003–5015.
- [12] S. Santra, P. R. Andreana, *Angew. Chem.* **2011**, *123*, 9590–9594; *Angew. Chem. Int. Ed.* **2011**, *50*, 9418–9422.
- [13] J. Yu, F. Shi, L.-Z. Gong, *Acc. Chem. Res.* **2011**, *44*, 1156–1171.
- [14] C. Gunanathan, M. Hçlscher, W. Leitner, *Eur. J. Inorg. Chem.* **2011**, 3381–3386.
- [15] R. A. Sheldon, H. van Bekkum, *Fine Chemicals through Heterogeneous Catalysis*, Wiley-VCH, Weinheim, **2007**, pp. 351–471.
- [16] A. R. Cartolano, G. A. Vedage, *Kirk-Othmer Encyclopedia of Chemical Technology*, Wiley, **2000**.
- [17] S. Horn, C. Gandolfi, M. Albrecht, *Eur. J. Inorg. Chem.* **2011**, 2863–2868.
- [18] T. D. Nixon, M. K. Whittlesey, J. M. J. Williams, *Tetrahedron Lett.* **2011**, *52*, 6652–6654.
- [19] P. S. Liu, *J. Org. Chem.* **1987**, *52*, 4717–4721.
- [20] T. T. Shawe, C. J. Sheils, S. M. Gray, J. L. Conard, *J. Org. Chem.* **1994**, *59*, 5841.
- [21] M. Periasamy, M. Thirumalaikumar, *J. Organomet. Chem.* **2000**, *609*, 137–151.
- [22] P. Baruah, M. P. Dutta, A. Baruah, D. Prajapati, J. S. Sandhu, *Synlett* **1999**, *4*, 409–410.
- [23] S. Kano, Y. Tanaka, E. Sugino, S. Hibino, *Synthesis* **1980**, *9*, 695–697.
- [24] C. Hoffman, R. S. Tanke, M. J. Miller, *J. Org. Chem.* **1989**, *54*, 3750–3751.
- [25] S. Itsuno, Y. Sakurai, K. Shimizu, K. Ito, *J. Chem. Soc. Perkin Trans. 1* **1989**, 1548–1549.
- [26] S. Itsuno, Y. Sakurai, K. Shimizu, K. Ito, *J. Chem. Soc. Perkin Trans. 1* **1990**, 1859–1863.
- [27] N. C. Smythe, J. C. Gordon, *Eur. J. Inorg. Chem.* **2010**, 509–521.
- [28] M. Rabinovitz, *The Cyano Group (1970)*, Wiley, **2010**, pp. 307–340.
- [29] A. Roucoux, J. Schulz, H. Patin, *Chem. Rev.* **2002**, *102*, 3757–3778.
- [30] J. O. Osby, S. W. Heinzman, B. Ganem, *J. Am. Chem. Soc.* **1986**, *108*, 67–72.
- [31] H. C. Brown, J. S. Cha, *J. Org. Chem.* **1993**, *58*, 3974–3979.
- [32] R. A. Michelin, M. Mozzon, R. Bertani, *Coord. Chem. Rev.* **1996**, *147*, 299–338.
- [33] N. Patel, R. Fernandes, A. Miotello, *J. Catal.* **2010**, *271*, 315–324.
- [34] U. B. Demirci, O. Akdim, J. Andrieux, J. Hannauer, R. Chamoun, P. Miele, *Fuel Cells* **2010**, *10*, 335–350.
- [35] J. M. Campelo, T. D. Conesa, M. J. Gracia, M. J. Jurado, R. Luque, J. M. Marinas, A. A. Romero, *Green Chem.* **2008**, *10*, 853–858.
- [36] C. Gonzalez-Arellano, R. Luque, D. J. Macquarrie, *Chem. Commun.* **2009**, 1410–1412.
- [37] V. Purcar, D. Donescu, C. Petcu, R. Luque, D. J. Macquarrie, *Catal. Commun.* **2009**, *10*, 395–400.
- [38] V. L. Budarin, J. H. Clark, R. Luque, D. J. Macquarrie, R. J. White, *Green Chem.* **2008**, *10*, 382.
- [39] J. M. Campelo, A. F. Lee, R. Luque, D. Luna, J. M. Marinas, A. A. Romero, *Chem. Eur. J.* **2008**, *14*, 5988–5995.
- [40] T. Mitsudome, Y. Mikami, K. Ebata, T. Mizugaki, K. Jitsukawa, K. Kaneda, *Chem. Commun.* **2008**, 4804–4806.
- [41] F. Alonso, P. Riente, M. Yus, *Tetrahedron* **2008**, *64*, 1847–1852.
- [42] T. Li, W. Zhang, R. Z. Lee, Q. Zhong, *Food Chem.* **2009**, *114*, 447–452.
- [43] M. J. Gracia, J. M. Campelo, E. Losada, R. Luque, J. M. Marinas, A. A. Romero, *Org. Biomol. Chem.* **2009**, *7*, 4821–4824.
- [44] L. Znak, J. Zielinski, *Appl. Catal. A* **2008**, *334*, 268–276.
- [45] R. W. J. Scott, O. M. Wilson, R. M. Crooks, *J. Phys. Chem. B.* **2005**, *109*, 692–704.
- [46] K. Esumi, R. Isono, T. Yoshimura, *Langmuir* **2004**, *20*, 237–243.
- [47] H. Xu, J. Xu, Y. Zhu, H. Liu, S. Liu, *Macromolecules* **2006**, *39*, 8451–8455.
- [48] A. Biffis, N. Orlandi, B. Corain, *Adv. Mater.* **2003**, *15*, 1551–1555.
- [49] J. Zhang, S. Xu, E. Kumacheva, *Adv. Mater.* **2005**, *17*, 2336–2340.
- [50] J. E. Wong, A. K. Gaharwar, D. Müller-Schulte, D. Bahadur, W. Richtering, *J. Colloid Interface Sci.* **2008**, *324*, 47–54.
- [51] M. Kuang, D. Wang, H. B. Bao, M. Y. Gao, H. Möhwald, M. Jiang, *Adv. Mater.* **2005**, *17*, 267–270.
- [52] Q. Sun, Y. Deng, *Langmuir* **2005**, *21*, 5812–5816.
- [53] L. Cen, K. G. Neoh, E. T. Kang, *Adv. Mater.* **2005**, *17*, 1656–1661.
- [54] M. R. Nabid, R. Sedghi, P. R. Jamaat, N. Safari, A. A. Entezami, *Appl. Catal. A* **2007**, *328*, 52–57.
- [55] M. R. Nabid, S. J. Tabatabaei Rezaei, *Appl. Catal. A* **2009**, *366*, 108–113.
- [56] M. R. Nabid, Y. Bide, S. J. Tabatabaei Rezaei, *Appl. Catal. A* **2011**, *406*, 124–132.
- [57] H. Ahmar, A. R. Fakhari, M. R. Nabid, S. J. T. Rezaei, Y. Bide, *Sens. Actuators B* **2012**, *171*–172, 611–618.
- [58] S. K. Sahu, A. Chakrabarty, D. Bhattacharya, S. K. Ghosh, P. Pramanik, *J. Nanopart. Res.* **2011**, *13*, 2475–2484.
- [59] Y. Lu, Y. Yin, B. T. Mayers, Y. Xia, *Nano Lett.* **2002**, *2*, 183–186.
- [60] P. Ball, L. Garwin, *Nature* **1992**, *355*, 761–766.
- [61] H. Takagi, H. Ogawa, Y. Yamazaki, A. Ishizaki, T. Nakagiri, *Appl. Phys. Lett.* **1990**, *56*, 2379–2380.
- [62] A. Ribera, I. Arends, S. de Vries, J. Perez-Ramirez, R. A. Sheldon, *J. Catal.* **2000**, *195*, 287–397.
- [63] J. A. Creighton, D. G. Eadon, *J. Chem. Soc. Faraday Trans.* **1991**, *87*, 3881–3891.
- [64] A. Curtis, D. Duff, P. Edwards, D. Jefferson, B. Johnson, A. Kirkland, A. Wallace, *J. Phys. Chem.* **1988**, *92*, 2270–2275.
- [65] A. L. Morel, S. I. Nikitenko, K. Gionnet, A. Wattiaux, J. Lai-Kee-Him, C. Labrugere, B. Chevalier, G. Deleris, C. Petibois, A. Brisson, M. Simonoff, *ACS Nano* **2008**, *2*, 847–856.
- [66] International XPS Spectral Data Processors, www.xpsdata.com.
- [67] N. R. Gleason, F. Zaera, *J. Catal.* **1997**, *169*, 365–381.
- [68] C. J. Collins, G. B. Fisher, A. Reem, C. T. Goralski, B. Singaram, *Tetrahedron Lett.* **1997**, *38*, 529–532.
- [69] H. C. Brown, K. C. Kim, S. J. Krishnamurthy, *J. Org. Chem.* **1980**, *45*, 1–12.
- [70] J. Malek, *Tetrahedron Lett.* **1968**, *9*, 3303–3306.
- [71] C. W. Jones, *Top. Catal.* **2010**, *53*, 942–952.
- [72] T. J. Yoon, J. S. Kim, B. G. Kim, K. N. Yu, M. H. Cho, J. K. Lee, *Angew. Chem.* **2005**, *117*, 1092–1095; *Angew. Chem. Int. Ed.* **2005**, *44*, 1068–1071.

Received: November 16, 2013

Published online on January 16, 2014